

Unusual doping induced phase transitions in NiS via solventless synthesis enabling superior bifunctional electrocatalytic activity

Ginena Bildard Shombe,¹ Malik Dilshad Khan,^{1*} Asma M. Alenad,² Jonghyun Choi,³ Tenzin Ingsel,³ Ram K. Gupta,³ Neerish Revaprasadu^{1*}

¹Department of Chemistry, University of Zululand, Private Bag X1001, KwaDlangezwa, 3886, South Africa.

²Department of Chemistry, College of Science, Jouf University, P.O. Box: 2014, Sakaka, Saudi Arabia.

³Department of Chemistry, Pittsburg State University, Pittsburg, KS 66762, USA.

*Email: RevaprasaduN@unizulu.ac.za; malikdilshad@hotmail.com

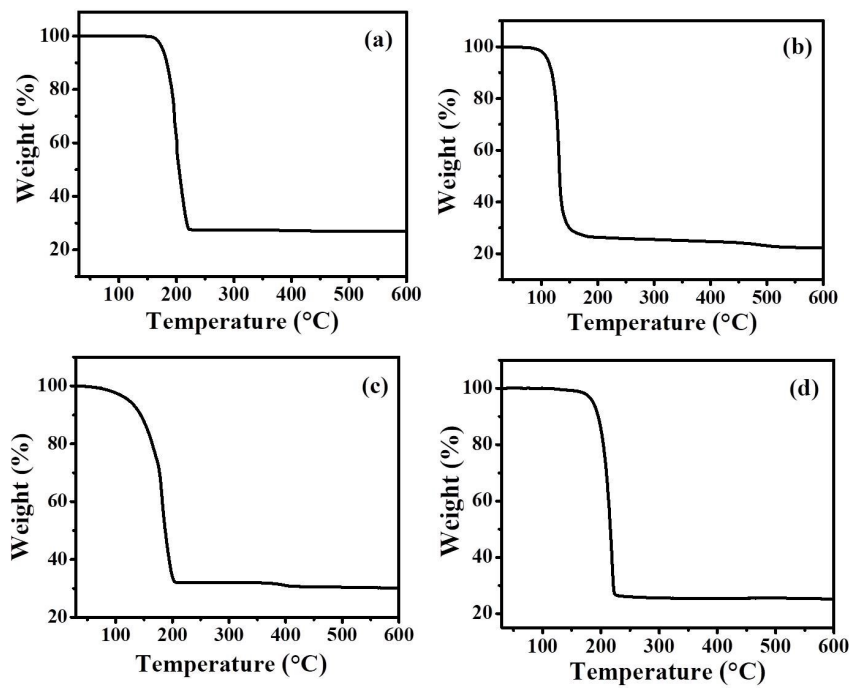


Figure S1. TG plots of (a) complex (1), (b) complex (2), (c) complex (3) and (d) complex (4).

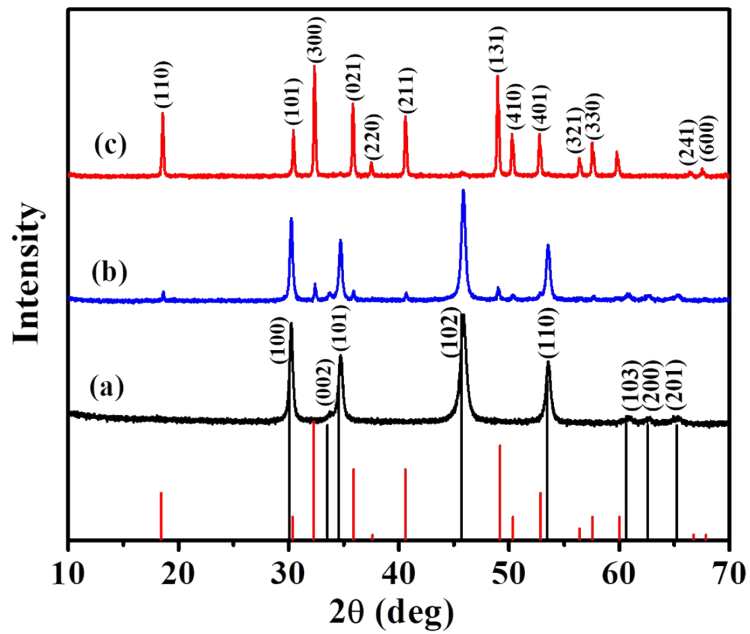


Figure S2. p-XRD patterns of NiS nanoparticles synthesized from complex (1) at (a) 200 °C (ICDD # 03-065-3419), (b) 300 °C and (c) 400 °C (ICDD # 00-003-0760).

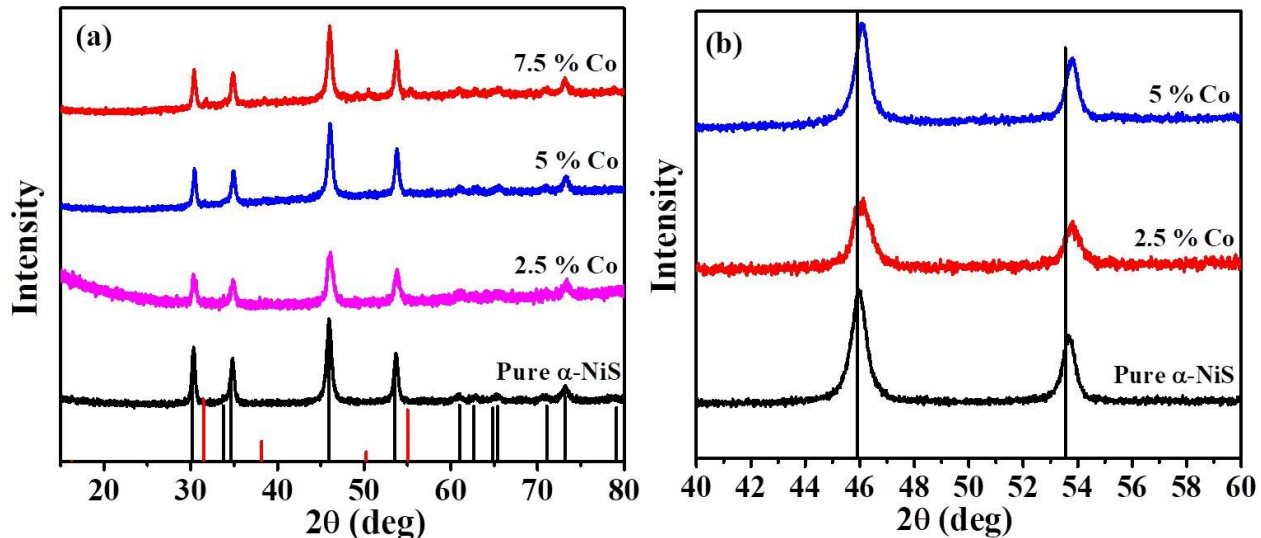


Figure S3. (a) p-XRD patterns of pure α -NiS and Co-doped α -NiS synthesized at 200 $^{\circ}\text{C}$. (b) Extended part of the diffraction patterns showing a shift in peak positions.

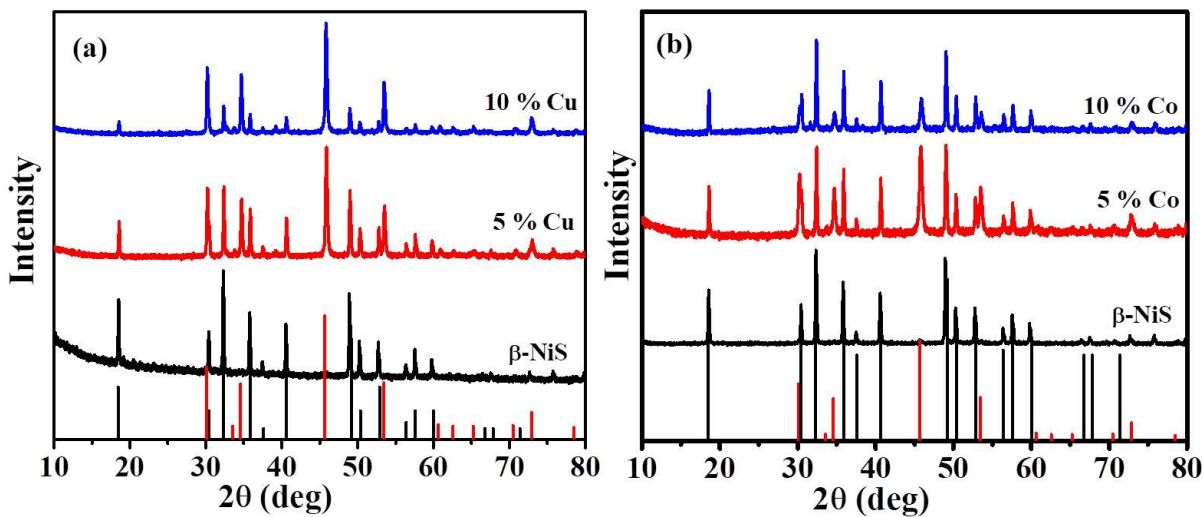


Figure S4. (a) p-XRD patterns of β -NiS and Cu-doped β -NiS synthesized at 400 $^{\circ}\text{C}$. (b) p-XRD patterns of β -NiS and Co-doped β -NiS synthesized at 400 $^{\circ}\text{C}$.

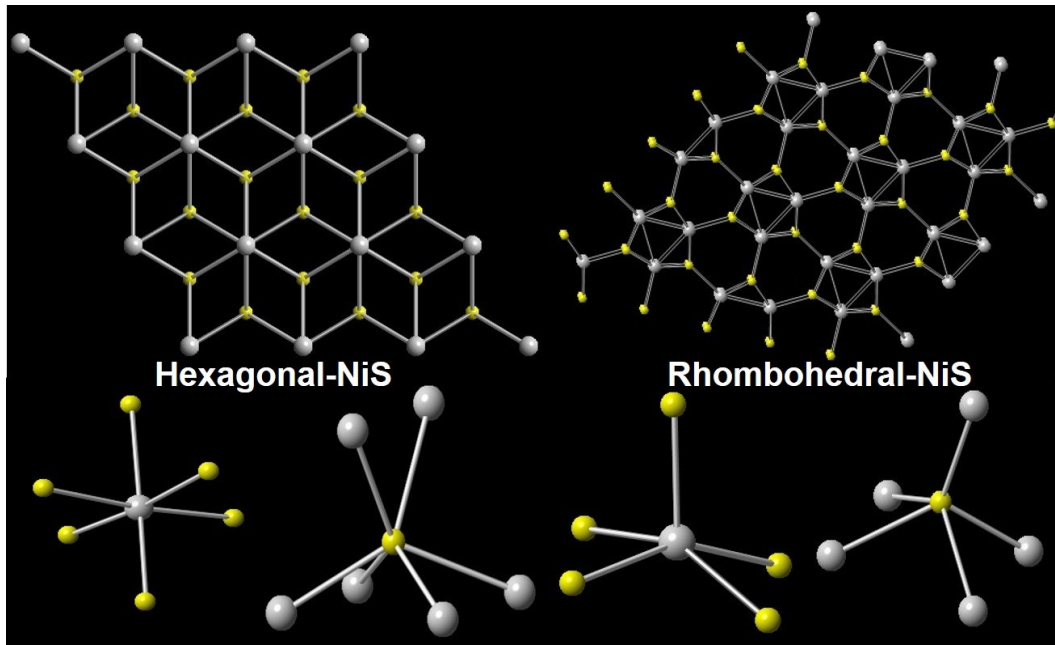


Figure S5. Crystal structures of hexagonal and rhombohedral NiS phases along with their respective nickel and sulfur coordination spheres.

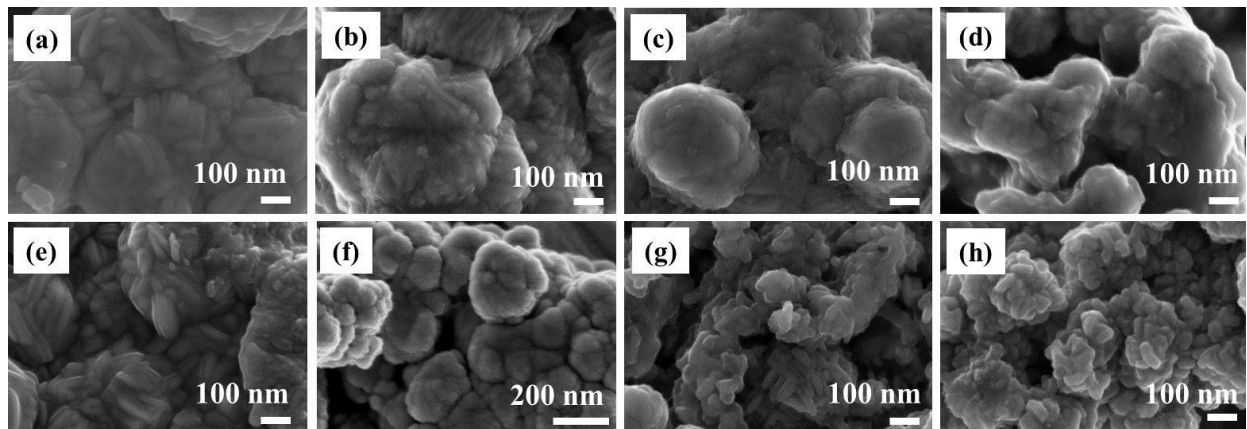


Figure S6. SEM images of (a) α -NiS (b) Cu-doped α -NiS, (c) Co-doped α -NiS, (d) Fe-doped α -NiS synthesized at 200 °C. SEM images of (e) β -NiS (f) Cu-doped β -NiS, (g) Co-doped β -NiS and (h) Fe-doped β -NiS synthesized at 400 °C.

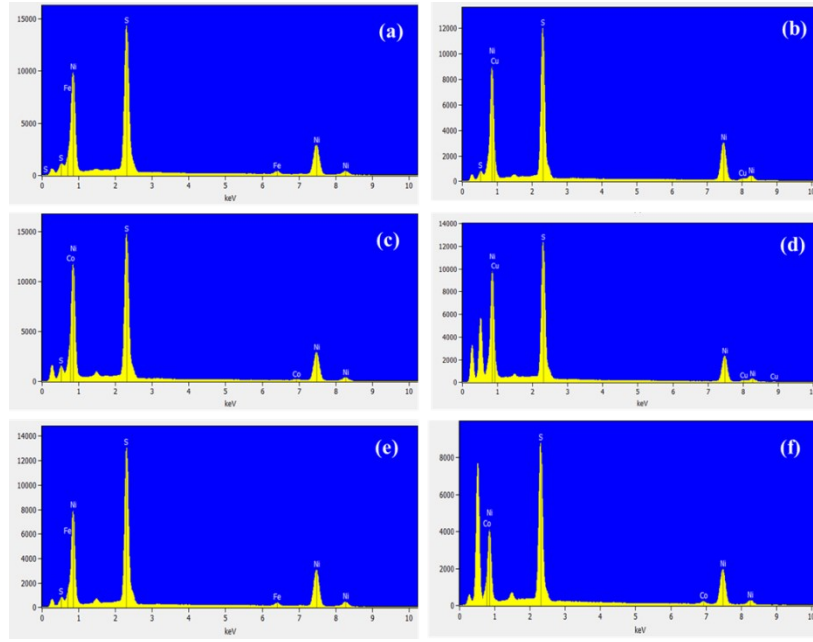


Figure S7. EDX spectra of (a) Fe-doped NiS, (b) Cu-doped NiS, and (c) Co-doped NiS synthesized at 200 °C; and (d) Cu-doped NiS, (e) Fe-doped NiS, and (f) Co-doped NiS synthesized at 400 °C.

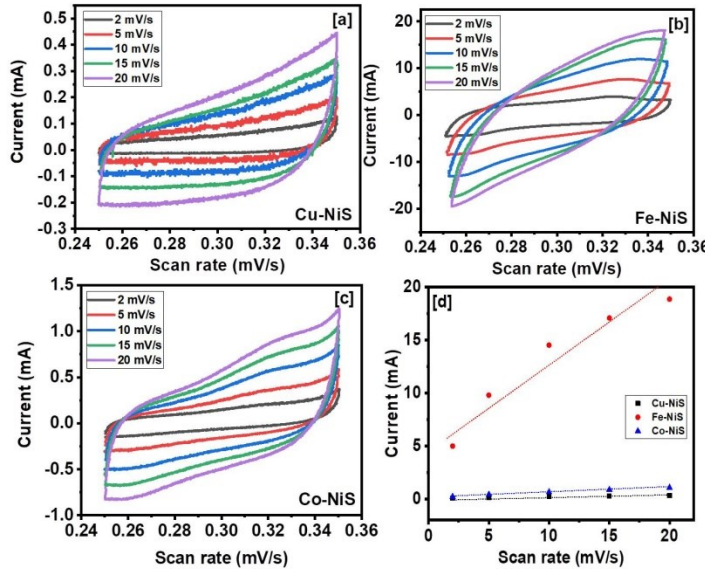


Figure S8. Double-layer capacitance measurements for estimating the electrochemically active surface area. CV curves in a non-Faradaic region for α -NiS doped with 5% (a) Cu (b) Fe and (c) Co. (d) Current vs scan rate plot for all the samples.

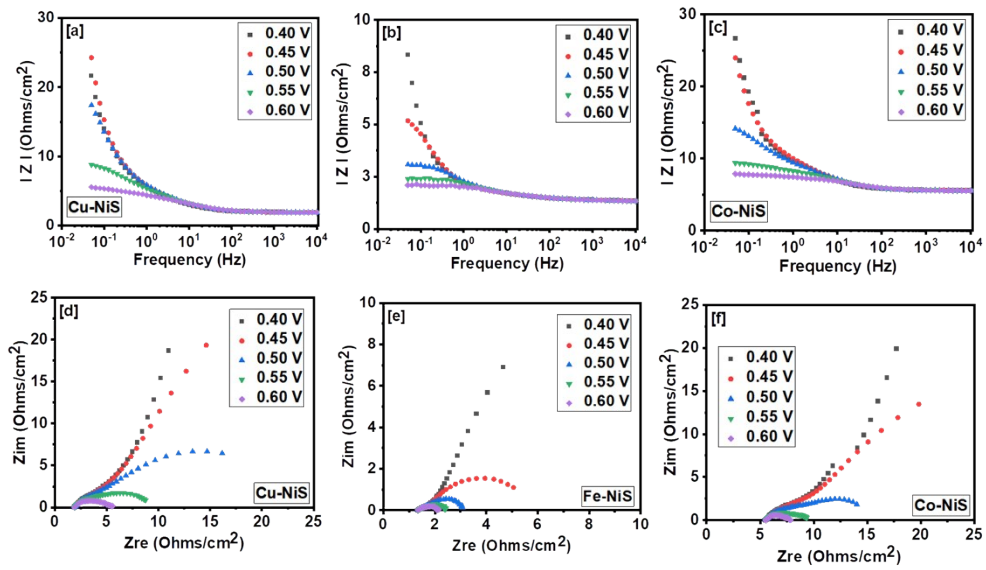


Figure S9. $|Z|$ vs. frequency plots for α -NiS doped with 5% (a) Cu (b) Fe and (c) Co at 200 °C. Z_{real} vs. Z_{img} plots at various potentials for NiS doped with 5% (d) Cu (e) Fe and (f) Co at 200 °C.

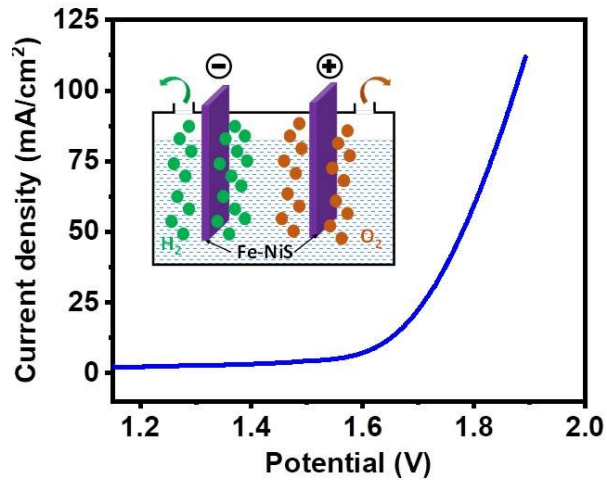


Figure S10. LSV curve for overall water splitting using Fe-doped NiS as both the cathode and anode.

Table S1. Atomic percent composition of Ni, S, Fe, Cu and Co in Fe-doped-, Cu-doped-, and Co-doped NiS synthesized at ^[a] 200 °C and ^[b] 400 °C.

| | Element | Required At% composition | Obtained At% composition |
|-----------------------------|---------|--------------------------|--------------------------|
| Fe-doped NiS ^[a] | Ni | 47.5 | 46.12 |
| | Fe | 2.5 | 2.60 |
| | S | 50 | 51.28 |
| Cu-doped NiS ^[a] | Ni | 47.5 | 46.23 |
| | Cu | 2.5 | 2.67 |
| | S | 50 | 51.10 |
| Co-doped NiS ^[a] | Ni | 47.5 | 46.36 |
| | Co | 2.5 | 2.57 |
| | S | 50 | 51.07 |
| Fe-doped NiS ^[b] | Ni | 45.0 | 46.13 |
| | Fe | 5.0 | 4.72 |
| | S | 50 | 49.15 |
| Cu-doped NiS ^[b] | Ni | 45.0 | 44.07 |
| | Cu | 5.0 | 4.93 |
| | S | 50 | 50.99 |
| Co-doped NiS ^[b] | Ni | 45.0 | 44.93 |
| | Co | 5.0 | 4.88 |
| | S | 50 | 50.19 |

Table S2. A comparison of the specific capacitance observed for TM-doped NiS with other Ni-based electrodes.

| Material | Method | Specific capacitance (F/g) | Current density (A/g) | Reference |
|------------------------------|--|----------------------------|-----------------------|-----------|
| α -NiS hollow spheres | Hydrothermal | 562.3 | 0.6 | [1] |
| β -NiS hollow spheres | Hydrothermal | 501.5 | 0.6 | [1] |
| β -NiS | Template assisted hydrothermal | 668 | 1 | [2] |
| β -NiS nanoflowers | Hydrothermal | 710 | 2 | [3] |
| β -NiS micro-flowers | Solvothermal | 857.76, 512.96 | 2, 5 | [4] |
| β -NiS/GO | Hydrothermal | 109 | 2.5 | [5] |
| NiS/rGO | Hydrothermal | 905.30 | 0.5 | [6] |
| NiS/C-dot | Hydrothermal | 880 | 2 | [3] |
| α -NiS/CRs | Solvothermal | 1092 | 1 | [7] |
| NiO nanowires | Nano-seed catalyzing mechanism | 180 | 0.5 | [8] |
| NiO/rGO | Electrophoretic and chemical bath deposition | 400 | 2 | [9] |
| NiO hollow spheres | Chemical bath deposition | 287 | 1 | [10] |

| | | | | |
|--|---|-------|-----|---------------------|
| NiCo ₂ S ₄ @MnO ₂ | Hydrothermal | 520.7 | 1 | [11] |
| NiCo ₂ S ₄ @Fe ₂ O ₃ | Hydrothermal followed by electro-deposition | 285 | 2.5 | [12] |
| Co-doped NiS | Solventless | 1586 | 0.5 | Present work |
| Cu-doped NiS | Solventless | 1326 | 0.5 | Present work |
| Fe-doped NiS | Solventless | 1314 | 0.5 | Present work |

Table S3. Comparison of HER performance of the synthesized TM-doped NiS with other Ni-based electrocatalysts.

| Catalyst | Overpotential (mV) at 10 mA/cm ² | Tafel Slope (mV/decade) | Reference |
|--|--|----------------------------|-----------|
| NiS | 474 | 124 | [13] |
| NiS ₂ | 454 | 128 | [13] |
| Ni ₃ S ₂ | 335 | 97 | [13] |
| Nitrogen doped-Ni ₃ S ₂ nanowires | 196 | 63 | [14] |
| NiS/Ni(OH) ₂ composite | 350 | 133 | [15] |
| Fe-NiS/Ni(OH) ₂ | 196 | 118 | [15] |
| NiS ₂ micro-architecture | 174 | 63 | [16] |
| NiS ₂ nanosheets array on carbon cloth (NiS ₂ NA/CC) | 243 | 69 | [17] |
| Ni ₃ S ₂ /Ni foam | 220 | 108 | [18] |

| | | | |
|---|-----|--------|---------------------|
| NiS ₂ /rGO | 200 | 52 | [19] |
| Hierarchically porous Ni ₃ S ₂ nanostructures | 200 | 107 | [20] |
| CoS _x /Ni ₃ S ₂ @NF | 204 | 133.32 | [21] |
| CoNi ₂ S ₄ | 255 | 85 | [22] |
| Fe-doped NiS | 146 | 113 | Present work |
| Cu-doped NiS | 154 | 114 | Present work |
| Co-doped NiS | 156 | 98 | Present work |

Table S4. Comparison of OER performance of the synthesized TM-doped NiS with other Ni-based electrocatalysts.

| Catalyst | Overpotential (mV) at 10 mA/cm ² | Tafel Slope (mV/decade) | Reference |
|---|--|----------------------------|-----------|
| NiS micro architectures | 320 | 59 | [16] |
| NiS@N/S-C nanocomposites | 417 | 48 | [23] |
| Ni ₃ S ₂ nanowires/Ni | 317 | 84.8 | [24] |
| NiO _x nanoparticles | 330 | 54 | [25] |
| Ni-P nanoparticles on Cu foam | 325 | 120 | [26] |

| | | | |
|---|--------|------|---------------------|
| NiCo ₂ O ₄ core-shell nanowires | 320 | 63.1 | [27] |
| Ni ₃ S ₂ NWs/Ni | 317 | 84.8 | [24] |
| Ni-Ni ₃ S ₂ /NF | 310 | 63 | [28] |
| Fe doped NiS | 266 mV | 79 | Present work |

References

- [1] C. Wei, C. Cheng, J. Zhao, Y. Wang, Y. Cheng, Y. Xu, W. Du, H. Pang, *Chemistry—An Asian Journal* **2015**, *10*, 679-686.
- [2] X. Y. Yu, L. Yu, L. Shen, X. Song, H. Chen, X. W. Lou, *Advanced Functional Materials* **2014**, *24*, 7440-7446.
- [3] S. Sahoo, A. K. Satpati, P. K. Sahoo, P. D. Naik, *ACS omega* **2018**, *3*, 17936-17946.
- [4] J. Yang, X. Duan, Q. Qin, W. Zheng, *Journal of Materials Chemistry A* **2013**, *1*, 7880-7884.
- [5] B. Prusty, M. Adhikary, C. Das, *Int. J. Curr. Res* **2014**, *6*, 7448-7452.
- [6] J. Yang, X. Duan, W. Guo, D. Li, H. Zhang, W. Zheng, *Nano Energy* **2014**, *5*, 74-81.
- [7] C. Sun, M. Ma, J. Yang, Y. Zhang, P. Chen, W. Huang, X. Dong, *Scientific reports* **2014**, *4*, 1-6.
- [8] H. Pang, Q. Lu, Y. Zhang, Y. Li, F. Gao, *Nanoscale* **2010**, *2*, 920-922.
- [9] X. Xia, J. Tu, Y. Mai, R. Chen, X. Wang, C. Gu, X. Zhao, *Chemistry—A European Journal* **2011**, *17*, 10898-10905.
- [10] X. Yan, X. Tong, J. Wang, C. Gong, M. Zhang, L. Liang, *Materials Letters* **2013**, *95*, 1-4.
- [11] H. Chen, X. L. Liu, J. M. Zhang, F. Dong, Y. X. Zhang, *Ceramics International* **2016**, *42*, 8909-8914.
- [12] R. Jia, F. Zhu, S. Sun, T. Zhai, H. Xia, *Journal of Power Sources* **2017**, *341*, 427-434.
- [13] N. Jiang, Q. Tang, M. Sheng, B. You, D.-e. Jiang, Y. Sun, *Catalysis Science & Technology* **2016**, *6*, 1077-1084.
- [14] F. Yu, H. Yao, B. Wang, K. Zhang, Z. Zhang, L. Xie, J. Hao, B. Mao, H. Shen, W. Shi, *Dalton Transactions* **2018**, *47*, 9871-9876.
- [15] T. A. Kandiel, *Applied Catalysis A: General* **2019**, *586*, 117226.
- [16] P. Luo, H. Zhang, L. Liu, Y. Zhang, J. Deng, C. Xu, N. Hu, Y. Wang, *ACS applied materials & interfaces* **2017**, *9*, 2500-2508.
- [17] C. Tang, Z. Pu, Q. Liu, A. M. Asiri, X. Sun, *Electrochimica Acta* **2015**, *153*, 508-514.
- [18] C. Tang, Z. Pu, Q. Liu, A. M. Asiri, Y. Luo, X. Sun, *International Journal of Hydrogen Energy* **2015**, *40*, 4727-4732.
- [19] R. Chen, Y. Song, Z. Wang, Y. Gao, Y. Sheng, Z. Shu, J. Zhang, X. a. Li, *Catalysis Communications* **2016**, *85*, 26-29.

- [20] C. Ouyang, X. Wang, C. Wang, X. Zhang, J. Wu, Z. Ma, S. Dou, S. Wang, *Electrochimica Acta* **2015**, *174*, 297-301.
- [21] S. Shit, S. Chhetri, W. Jang, N. C. Murmu, H. Koo, P. Samanta, T. Kuila, *ACS applied materials & interfaces* **2018**, *10*, 27712-27722.
- [22] D. Wang, X. Zhang, Z. Du, Z. Mo, Y. Wu, Q. Yang, Y. Zhang, Z. Wu, *International Journal of Hydrogen Energy* **2017**, *42*, 3043-3050.
- [23] L. Yang, M. Gao, B. Dai, X. Guo, Z. Liu, B. Peng, *Electrochimica Acta* **2016**, *191*, 813-820.
- [24] D. Zhang, J. Li, J. Luo, P. Xu, L. Wei, D. Zhou, W. Xu, D. Yuan, *Nanotechnology* **2018**, *29*, 245402.
- [25] L.-A. Stern, X. Hu, *Faraday discussions* **2015**, *176*, 363-379.
- [26] Q. Liu, S. Gu, C. M. Li, *Journal of Power Sources* **2015**, *299*, 342-346.
- [27] R. Chen, H.-Y. Wang, J. Miao, H. Yang, B. Liu, *Nano Energy* **2015**, *11*, 333-340.
- [28] N. K. Chaudhari, A. Oh, Y. J. Sa, H. Jin, H. Baik, S. G. Kim, S. J. Lee, S. H. Joo, K. Lee, *Nano Convergence* **2017**, *4*, 7.